CHARACTERISTICS OF MOMENTUM SOURCES AND SINKS IN TURBULENT CHANNEL FLOW

J. P. Monty[1] **& J. C. Klewicki**[2]
Department of Mechanical Engineering,
University of Melbourne,
Parkville, Australia
[1]montyjp@unimelb.edu.au
[2]klewicki@unimelb.edu.au

B. Ganapathisubramani
Faculty of Engineering & Environmnent,
University of Southampton
Highfield, Southampton, SO17 1BJ, UK
g.bharath@soton.ac.uk

ABSTRACT

The wall-normal gradient of Reynolds shear stress, denoted $\partial T^+/\partial y^+$, may be thought of as a momentum source or sink term (depending on its sign). This quantity represents a critical driver of the dynamics of wall-turbulence that give rise to the mean velocity distribution. While there have been a number of studies concerning the statistics of $\partial T^+/\partial y^+$, there remains much to discover regarding the flow features and their interactions that contribute to $\partial T^+/\partial y^+$. The aim of the present work is to investigate the velocity–vorticity correlations that comprise the Reynolds shear stress gradient. Results show velocity–vorticity correlations rapidly change behaviour up to the location of peak Reynolds shear stress. Beyond this point, the qualitative behaviour remains similar throughout the turbulent flow. Interestingly, it was found from two-point correlations that the mean Reynolds stress gradient at any wall-normal location results from only slight asymmetry in the velocity–vorticity correlations. This suggests that the mean momentum balance is extremely sensitive to the structural features and/or interactions that are responsible for vorticity transport throughout the turbulent layer.

INTRODUCTION

The complexity of the Navier-Stokes equations poses well-known obstacles to the theoretical and computational study of fluid dynamics, particularly in the case of wall-bounded turbulent flows. For the case of turbulent flows over surfaces, the Reynolds averaged Navier-Stokes equation in the streamwise direction, for nominally two-dimensional flow, is given by,

$$U\frac{\partial U}{\partial x}+V\frac{\partial U}{\partial y}=-\frac{1}{\rho}\frac{\partial p}{\partial x}+\nu\frac{\partial^2 U}{\partial y^2}-\frac{\partial \overline{uv}}{\partial y} \qquad (1)$$

where, p is the pressure, ρ is the density of the fluid, (U,V,W) and (u,v,w) are the mean and fluctuating velocities along streamwise, wall-normal and spanwise (x,y,z) directions, respectively. This equation reflects the mean differential statement of Newton's second law. For consistency with recent relevant publications that have explored the properties of (1), we denote $-\overline{uv}$, as T. Together with continuity, (1) can be solved as a regular boundary value problem if, for example, $T(x,y)$ is known, or, equivalently, if a supplementary equation that relates T to U can be determined. The challenges to solving (1) constitute the wall-turbulence version of the broader *closure* problem of turbulence, and significant research has gone into developing models for T.

Herein we consider (1) for the case of fully developed planar channel flow. This equation can be made dimensionless by normalizing with a velocity scale, U_τ and length scale, ν/U_τ (where ν is the kinematic viscosity, $U_\tau=\sqrt{\tau_w/\rho}$ is the friction velocity and τ_w is the wall shear stress). Under the fully developed condition, the left side of (1) is identically zero, and the mean non-dimensional differential statement of dynamics becomes,

$$0=\frac{1}{\delta^+}+\frac{d^2U^+}{dy^{+2}}+\frac{dT^+}{dy^+} \qquad (2)$$

where δ is the channel half-height and δ^+ is the Kármán number. Wei *et al.* (2005) empirically documented and theoretically analysed the properties of (2) using direct numerical simulation (DNS) data. They revealed the existence of a four-layer structure, and determined the Reynolds number scaling properties associated with these layers. This layer structure is defined using the magnitude ordering of the terms in (2). The dT^+/dy^+ term was shown to be of leading order in three of the four layers.

The wall-normal variation of the position, y_m^+, at which $T(=-\overline{uv})$ attains its single maximum value has long been

the topic of investigation in wall-bounded flows Long & Chen (1981); Afzal (1982); Sreenivasan & Sahay (1997); Wei *et al.* (2005). Of course, dT^+/dy^+ also passes through zero at y_m^+. Consequently, when viewed as a force, the dT^+/dy^+ term acts like a mean momentum source for $y^+ < y_m^+$ (where $dT^+/dy^+ > 0$) and a momentum sink for $y^+ > y_m^+$ (where $dT^+/dy^+ < 0$). These findings support a view of the mean effect of turbulent inertia that is distinctly different from the long-held view that essentially any positive value of $-\overline{uv}^+$ contributes to positive momentum transport (also see Klewicki et al. (2007); Eyink (2008)). A present aim is to reveal basic attributes of the velocity and vorticity field interactions that underlie the source/sink properties of dT^+/dy^+.

This aim is furthered by noting that, for the given flow, dT^+/dy^+ is exactly expressed as the difference of velocity vorticity correlations (see Tennekes & Lumley 1972):

$$\frac{dT^+}{dy^+} = \overline{v\omega_z}^+ - \overline{w\omega_y}^+ \tag{3}$$

where ω_i ($i = x,y,z$) denote the fluctuating components of vorticity along (x, y, z) directions. There are a number of intriguing features associated with (3). Perhaps most notable is that the mean effect of turbulent inertia is described by the difference of correlations between field variables that are generally considered to concentrate at disparate wavenumbers (velocity and vorticity, respectively) – and increasingly so as $\delta^+ \to \infty$. This motivates inquiry into which scales of motion determine the scaling behaviours of the terms in (3).

Guala, Hommema & Adrian (2006) computed the wall-normal derivative of the uv co-spectra in a pipe flow across the outer region (layer IV). From these measurements they concluded that, in this region, the very-large scale motions (VLSMs) contribute significantly. Similarly, McKeon & Sharma (2011) recently developed a critical layer model for turbulent pipe flow. In this they treat the dT^+/dy^+ term as an unknown forcing. The results of their model indicate a linear relationship between the velocity field response and the nonlinear mechanism of turbulent. They further found that this model provided some encouragingly realistic descriptions of the properties of the turbulent fluctuations – especially those affiliated with the large-scale motions. While this method holds promise, the underlying physical mechanisms for momentum transport (affiliated with dT^+/dy^+) remain hidden (embedded).

In apparent contrast to the findings of Guala, Hommema & Adrian (2006) and McKeon & Sharma (2011), studies that have directly quantified the velocity-vorticity correlations on the right of (3) generally indicate that the small-scale (vorticity field) motions are important at essentially all positions across the layer, and especially so as the wall is approached. These studies include Klewicki (1989), Crawford and Karniadakis (1997), Rovelstadt (1991) and Ong (1992), all of which revealed nominally consistent results. Notably, the results of Ong (1992) also indicated that the simultaneously measured combinations of ω_z and ω_y are statistically consistent with the lifting of hairpin-like vortices. Rajagopalan & Antonia (1993) studied the structure of velocity field associated with the spanwise vorticity field and reported cross correlations of $v\omega_z$ and $u\omega_z$. They concluded that the velocity signature is consistent with the presence of internal shear layers, inclined to the wall. Klewicki, Murray & Falco (1994) investigated the $v\omega_z$ term in the near wall region and concluded that the existence of positive spanwise vorticity for $y^+ > 12$, and that its regular pairing with motions bearing negative ω_z is consistent with the presence of a ring-like eddy, but that other possibilities exist as well. Klewicki & Hirsch (2004) analyzed combined hotwire/flow visualisation measurements near the wall and found that $v\omega_z$ local to near-wall shear layers produces contributions to the Reynolds stress gradient that are attenuated relative to their local mean values.

The above cited studies indicate that the structure of the mechanisms involved in the balance of terms in (3) involve complex interactions between quantities that span significant wavenumber ranges. The evolution of these interactions with increasing δ^+ and increasing y^+ (at any given δ^+) are not well-understood. In connection with this, the boundary layer study of Priyadarshana *et al.* (2007) discovered the existence of a *scale-selection* phenomena in which the primary contributions to the resulting correlation comes from narrow wavenumber ranges centered about the spectral peaks of the individual participating velocity and vorticity components. For the near-wall motions this scale-selection is consistent with the velocity field *induced* by concentrated vortical motions. For the motions away from the wall, Priyadarshana *et al.* (2007) proposed a model, consistent with the initial observations of Meinhart & Adrian (1995), in which the approximately uniform momentum zones (affiliated with the VLSMs) are intermittently segregated by advecting vortical fissures. Further analyses show that the scale selection phenomena varies in a consistent way with distance from the wall, and provide evidence that scale separation between the relevant velocity and vorticity components is a well-defined (and potentially universal) function of the distance from the wall. The results of Ganapathisubramani (2008) add further insight in this regard by exploring the spatial structure of dT^+/dy^+ using dual-plane PIV measurements. These measurements were acquired in the outer region of a turbulent boundary layer (where dT^+/dy^+ exhibits its momentum sink-like behaviour), and revealed that instantaneous source-like motions are correlated with elongated low momentum zones that possess regions of up-wash embedded within it. These motions appear to be the strongest in areas where the low momentum zones meander in the spanwise direction. Conversely, the instantaneous momentum sinks appear to be located within "lower" speed regions that are embedded within larger high momentum zones. This investigation also revealed a strong scale dependence with distance from the wall in the motions that contribute to dT^+/dy^+.

As motivated by the above review, herein we explore the spatial structure of the terms in (3) in a turbulent channel flow at $\delta^+ = Re_\tau = 934$. Relative to interpretations of the underlying physical and mathematical structure, we draw upon the *attached eddy* model of Townsend (Townsend (1976); Perry & Chong (1982); Perry & Marusic (1995)) and the analyses of (2) by Fife and co-workers (Wei *et al.* (2005); Fife et al. (2005, 2009)). Both of these approaches provide a hierarchy based description of the underlying motions, while the analyses of Fife et al. draw explicit mathematical connections between the dynamical self-similarities admitted by (2), the mean mechanism of turbulent inertia, dT^+/dy^+, and a hierarchical structure that asymptotically scales with distance from the wall.

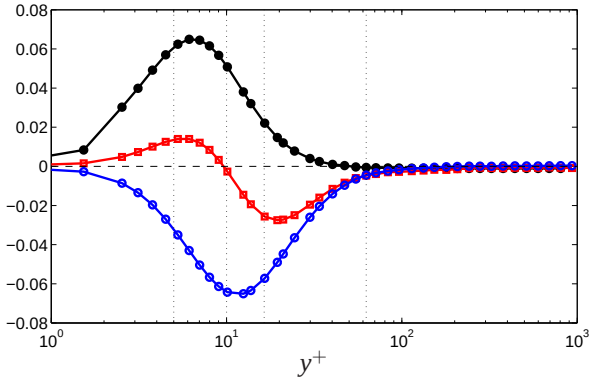

Figure 1. Wall-normal profiles of the terms in (3) at $\delta^+ = 934$. dT^+/dy^+, black line; $\overline{v\omega_z}^+$, red line; $\overline{w\omega_y}^+$, blue line.

RESULTS

In this study, we examine the characteristics of individual terms in equation (3) by interrogating the Direct Numerical Simulation (DNS) data of turbulent channel flow at $\delta^+ = 934$ by del Alamo *et al.* (2004). Figure 1 shows the terms in (3). As indicated, $\partial T^+/\partial y^+$ exhibits a spatially localized and large positive peak near $y^+ = 7$, passes through zero (at $y_m^+ \approx 60$) and exhibits low amplitude negative values for $y^+ > y_m^+$. Relative to interpreting the source and sink contributions of the motions reflected in figure 1, it is important to keep in mind that the area under the dT^+/dy^+ profile is zero, and thus the total source and sink contributions to dT^+/dy^+ are identically equal for all δ^+.

The velocity-vorticity correlations of figure 1 display a number of significant features. The $\overline{w\omega_y}^+$ profile is largely of a single (negative) sign, exhibiting a distinct peak near $y^+ = 12$ and decaying to an amplitude close to zero for $y^+ > y_m^+$. As $y^+ \to \delta^+$, $\overline{w\omega_y}^+$ crosses zero and attains a constant value close to zero but between zero and $1/\delta^+$. Conversely, the $\overline{v\omega_z}^+$ profile exhibits two distinct peaks (one positive, one negative) in the near-wall region $y^+ < 20$. The positive peak near $y^+ = 6$ is about half the amplitude of the negative peak near $y^+ = 19$, while the zero-crossing of this profile is near $y^+ = 10$. This function then decays to a constant negative value that is close to, but less than $1/\delta^+$ at $y^+ = \delta^+$. Of course, as demanded by (3), profiles of $\overline{w\omega_y}^+$ and $\overline{v\omega_z}^+$ cross each other at y_m^+.

Relative to its interpretation as a momentum source or sink, the data of figure 1 indicate that interior to its zero-crossing $\overline{v\omega_z}^+$ represents a source contribution, and for all greater distances from the wall it acts like a momentum sink. Conversely, $\overline{w\omega_y}^+$ acts like a source out to about $\delta^+/4$, and like a sink for greater y^+. Physically, one can rationally associate the positive values of $\overline{v\omega_z}^+$ in and near the viscous sublayer with the lifting of low speed (positive ω_z fluctuation) streaks. For $y^+ \gtrsim 10$ the negative $\overline{v\omega_z}^+$ correlation is similarly associated with the outward transport of motions bearing negative ω_z fluctuations – the primary candidate (at least near the wall) being the *heads* of hairpin-like vortices. Over the region in which this profile is negative, the $\overline{w\omega_y}^+$ correlation is consistent with the action by which the *legs* of hairpin-like vortices are stretched as the motion evolves away from the wall. The veracity of these interpretations is clarified further via examination of the spatial correlations below.

Per the scaling analysis of Tennekes & Lumley (1972), one can nominally associate the $\overline{v\omega_z}^+$ correlation with the wall-normal transport of ω_z, while the $\overline{w\omega_y}^+$ correlation can be largely associated with *change of scale* effects owing to vortex stretching. In light of the interpretations above, these scaling arguments would seem to hold some validity. For example, both empirical and theoretical analysis of (2) reveals that for $y^+ > y_m^+$ (or more precisely, at the onset of layer IV in the four layer structure described by Wei *et al.* 2005) the leading order mean dynamics are increasingly well-described by a balance between the mean effect of turbulent inertia, dT^+/dy^+, and the mean pressure gradient, $1/\delta^+$. As indicated by figure 1, beyond this position is also where $|\overline{v\omega_z}^+|$ exceeds $|\overline{w\omega_y}^+|$. In accord with both the inviscid attached eddy model, and the direct analysis of (2), this region is where the distance-from-the-wall scaling should be most rapidly approximated. Thus, in connection with the analysis of spatial structure below, these predict that the correlations should begin to exhibit scale dependence on distance from the wall at $y^+ \simeq 2.6\sqrt{\delta^+}$ or $\simeq 80$ at the present Reynolds number.

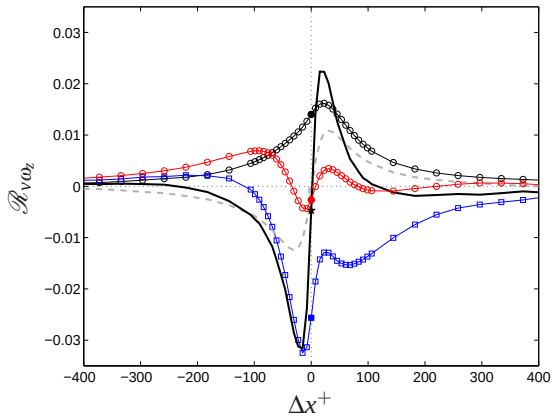

Figure 2. Streamwise two-point correlation of wall-normal velocity and spanwise vorticity. ∘, $y^+ = 5$; ∘, $y^+ = 10$; □, $y^+ = 16.5$; —, $y^+ = 60$; −−, $y^+ = 324$. Solid symbols highlight value at zero streamwise separation (i.e., $\overline{v\omega_z}$).

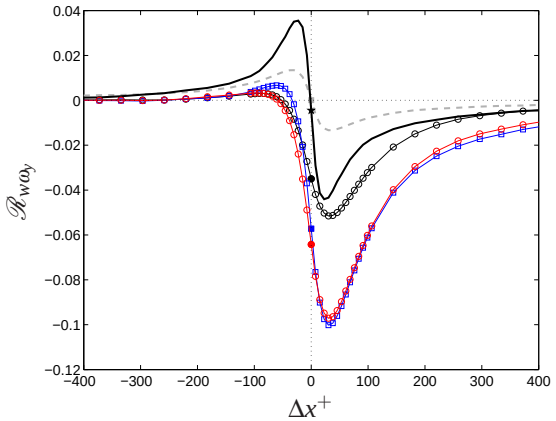

Figure 3. Streamwise two-point correlation of spanwise velocity and wall-normal vorticity. Symbols as in figure 2.

Figures 2 and 3 respectively present the inner-normalized two-point correlations of $\mathscr{R}_{v\omega_z} = \overline{\omega_z(x)v(x+\Delta x)}^+$ and

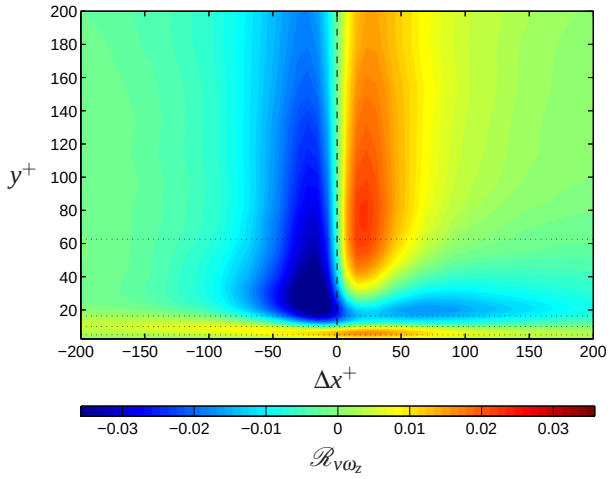

Figure 4. Contour map of streamwise two-point correlations of wall-normal velocity and spanwise vorticity for a range of y^+. Dotted lines indicate locations of selected correlations shown in previous figures.

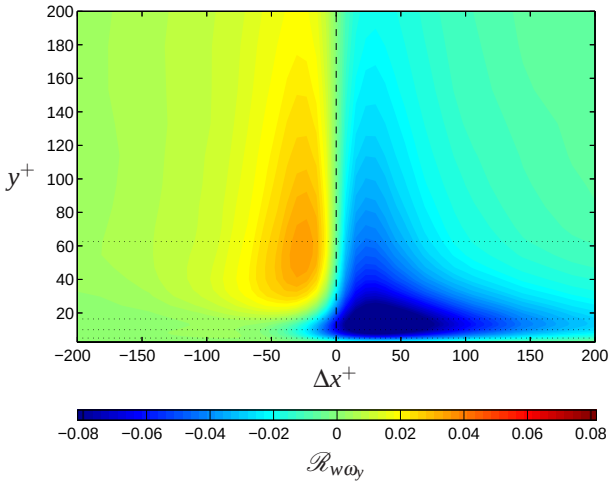

Figure 5. Contour map of streamwise two-point correlations of spanwise velocity and wall-normal vorticity.

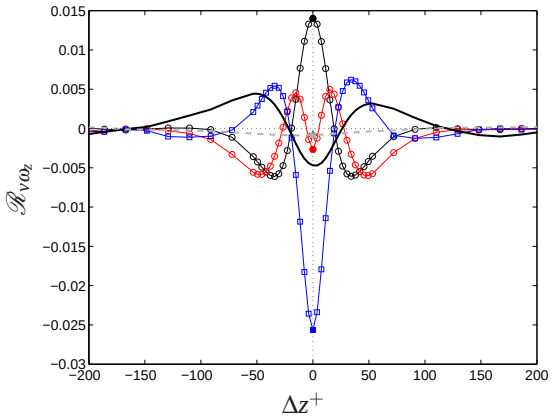

Figure 6. Spanwise two-point correlation of wall-normal velocity and spanwise vorticity. Symbols as in figure 2.

$\mathscr{R}_{w\omega_y} = \overline{\omega_y(x)w(x+\Delta x)}^+$. Very near the wall, the $\mathscr{R}_{v\omega_z}$ correlation is strictly positive, and has a nearly symmetric shape around $\Delta x^+ = 0$, with the peak value occurring at only a small positive Δx. With increasing distance from the wall, however, this correlation shifts to nearly wholly negative values, and develops rather strong asymmetries about $\Delta x^+ = 0$. By the position of y_m^+ these asymmetries are strongly diminished, rendering the resulting correlation at $\Delta x^+ = 0$ the result of a slight shift in the zero-crossing between two well-defined peaks (negative then positive) at $\pm\Delta x^+ \simeq 15$. In contrast, the sequence of correlation curves in figure 3 all exhibit a similar shape, that is characterized by a pronounced negative peak at positive Δx^+. With increasing distance from the wall these curves gradually develop a distinct positive peak at small negative Δx^+. As with the $\mathscr{R}_{v\omega_z}$ correlation, by y_m^+ the $\mathscr{R}_{w\omega_y}$ correlation curve is characterized by positive and negative peaks spaced about $30\Delta x^+$ apart, and displaying only a slight asymmetry relative to $\Delta x^+ = 0$. Interestingly, the curves of figures 2 and 3 near y_m^+ both display shapes that are respectively consistent with the correlation expected from the passage of isolated vortices bearing ω_z and ω_y. Beyond y_m^+ the shape of the two-point correlations changes only marginally, although the overall correlation magnitude decreases with increasing y^+.

An over-arching attribute of all of the correlations in figures 2 and 3 is that the value at $\Delta x^+ = 0$ (i.e., the value that contributes to the net dynamical effect in equation 2) is less than, and regularly significantly less than, the values of the maximal value of the spatially delayed correlation. This is taken to indicate that, in a statistical sense, significantly distinct dynamical states can be generated by only small modifications to the underlying velocity and vorticity field interactions. This notion would seem to find support from recent findings in polymer drag reduced channel flows (Kim et al. 2007; White et al. 2011).

The wall-normal variation of the streamwise correlation can be further explored by stacking the correlations across all accessible wall-normal locations. Figures 4 and 5 show contour maps of $\mathscr{R}_{v\omega_z}(\Delta x^+, y^+)$ and $\mathscr{R}_{w\omega_y}(\Delta x^+, y^+)$, respectively. The above-mentioned asymmetries in the correlations can be clearly seen in these figures. Figure 4 shows that the correlation remains positive across the entire streamwise length near the wall and becomes negative for the entire streamwise length beyond $y^+ \approx 15$. The correlation remains negative along the entire length up to a wall-normal location of $y^+ \approx 30$ beyond which the correlation for $\Delta x^+ > 0$ starts to becomes positive. Beyond this location, the correlations is positive for $\Delta x > 0$ and negative for $\Delta x < 0$. This feature is also apparent in $\mathscr{R}_{w\omega_y}$ correlation where the correlation is negative for $\Delta x > 0$ and is positive for $\Delta x < 0$ beyond $y^+ \approx 30$. This is consistent with the passage of a isolated vortices bearing ω_z and ω_y. This signature becomes relatively stronger (increasing peak values) and larger (extends to larger streamwise distances) with increasing distance from the wall. This is consistent with Townsend's attached eddy hypothesis.

Figures 6 and 7 respectively present the inner-normalized two-point correlations in the spanwise direction of $\mathscr{R}_{v\omega_z} = \overline{\omega_z(z)v(z+\Delta z)}^+$ and $\mathscr{R}_{w\omega_y} = \overline{\omega_y(z)w(z+\Delta z)}^+$. At $y^+ = 5$, the $\mathscr{R}_{v\omega_z}$ is positive at the origin and falls off to a negative value, crossing zero at $\Delta z^+ \approx 20$ and reaching a minimum value (whose magnitude is approximately half of the magnitude at the origin) at $\Delta z^+ \approx 30$. The correlation is symmetric about $\Delta z^+ = 0$. With increasing distance from the wall, the correlation retains its symmetry about $\Delta z^+ = 0$, however,

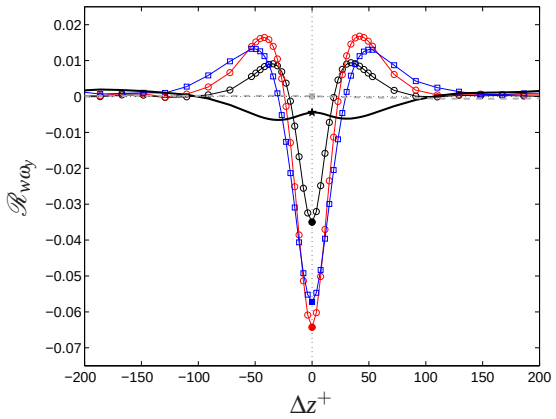

Figure 7. Spanwise two-point correlation of spanwise velocity and wall-normal vorticity. Symbols as in figure 2.

the shape of the correlation curves is significantly altered. At $y^+ = 10$, the correlation has 5 local maxima/minima. This includes a negative local peak at the origin, a local positive peak at $\Delta z^+ \simeq \pm 15$ and a local negative peak again at $\Delta z^+ \simeq \pm 40$. This suggests rapid velocity-vorticity interaction at this wall-normal location with multiple sign changes in the value of the correlation. Farther away from the wall, correlation at the origin remains negative, however, there are only two other positive peaks. The spanwise distance between these positive peaks increases with increasing wall-normal distance suggesting a scale growth in the spanwise direction with wall-normal location.

As dictated by the 1-D nature of the mean flow, the two-point correlations in the spanwise direction are in figures 6 and 7 are symmetric about $\Delta z^+ = 0$. Overall, it also revealed that the spanwise extent of the velocity vorticity correlations is significantly smaller than their streamwise extent. Consistent with the wall-normal transport of positive ω_z from the sublayer (as affiliated with the lifting of streaks), the $R_{v\omega_z}(z+\Delta z)$ correlation near $y^+ = 5$ exhibits a large positve peak near $\Delta z^+ = 0$ that is symmetrically flanked by negative correlation peak near $\Delta z^+ = \pm 50$. When lifted from the wall, positive $\omega_z$motions in the sublayer rapidly become negative fluctuations owing to the precipitous drop in the mean vorticity profile with increasing y^+. These (or similar) physics explain the loss of positive correlation near $\Delta z^+ = 0$, while the rapid development of a negative peak centered about $\Delta z^+ = 0$ and flanked by weaker positive peaks is consistent with the outward motion of the heads of hairpin-like vortices. The negative peak weakens considerably with wall-normal distance, while the flanking positive peaks weaken and spread. As in figure 3, the near-wall profiles of figure 7 are largely consistent with the flow field local to a wall-normal oriented vortex bearing either positive or negative ω_y. By y_m^+, however, the qualitative behavior of the correlation changes; losing both its strong negative peak near $\Delta z^+ = 0$ and its positive flanks.

All of the data examined thus far are consistent with the region interior to y_m^+ being populated with organized vortical motions that arise out of the *reservior* of spanwise vorticity that exists in the region $y^+ \lesssim 10$. As evidenced by the relative magnitudes of the $\overline{v\omega_z}^+$ and $\overline{w\omega_y}^+$ contributions to dT^+/dy^+, this region is marked by intense vortex stretching of ω_y in concert with the outward transport of ω_z. As mentioned previously, these observations are consistent with the dynamical evolution of hairpin-like vortices (i.e., the outward transport is affiliated with the hairpin vortex heads and the stretching with their legs). With the crossing of the $\overline{v\omega_z}^+$ and $\overline{w\omega_y}^+$ profiles at y_m^+, the qualitative behaviors of the momentum and vorticity field mechanisms qualitatively change. Namely, there is a correspondence between the emergence of the vorticity transport contribution in (3) simultaneous with the loss of the viscous force as a dominant order term in (2).

Under the condition of an inertially dominated mean flow, the attached eddy model predicts (e.g., see Perry & Chong (1982); Perry & Marusic (1995)) a distance from the wall scale dependence in the underlying motions. Additionally, multi-scale analysis (e.g., Fife et al. (2009) shows that (2) admits an invariant (universal) form when scaled by a characteristic length that explicitly depends on the decay rate of dT^+/dy^+. This length scale becomes an increasingly linear function of y as $\delta^+ \to \infty$. From the two-point correlation data it is possible to define length scales. A streamwise length scale was determined as the spacing of the two-point correlation crossing the thresholds of ± 0.33 multiplied by the peak correlation value at a given wall-normal location. A spanwise length scale was determined as the spacing between the two-point correlations as they cross the threshold of 0.33 multiplied by the minimum correlation value. The results are plotted in figure . The streamwise length scales indicate a clear linear dependence on wall-distance in both lamb vector components. In the spanwise direction, the picture is not quite so clear, however, it is difficult to uniquely determine a length scale in this direction since the shapes of the two-point correlations are complex and vary rapidly. Also, there is less overall correlation in the spanwise direction compared with the streamwise direction for large wall-distances. In any case, it is evident that the spanwise extent of contributions to the velocity–vorticity correlations increases with y^+ in a roughly linear manner.

Conclusions

In this paper, velocity-vorticity correlations are examined in a turbulent channel flow to understand the influence of turbulent inertia on the mean-momentum balance. Results show that the correlations between spanwise velocity and wall-normal vorticity and between wall-normal velocity and spanwise vorticity, rapidly change behaviour up to the location of peak Reynolds shear stress. Beyond this point, the qualitative behaviour remains similar. The velocity–vorticity two-point correlations in the streamwise direction reveal only a slight asymmetry about $\Delta x^+ = 0$. This suggests that the mean Reynolds stress gradient at any wall-normal location is a direct result of a slight asymmetry in the characteristic vortical motions of the flow. This suggests that the mean momentum balance is sensitive to the structural features and/or interactions that are responsible for vorticity transport throughout the turbulent layer. From a flow control perspective, this is a significant result as it implies that a small change to the asymmetry of the velocity–vorticity correlations could result in large changes in the mean flow field, particularly close to the wall.

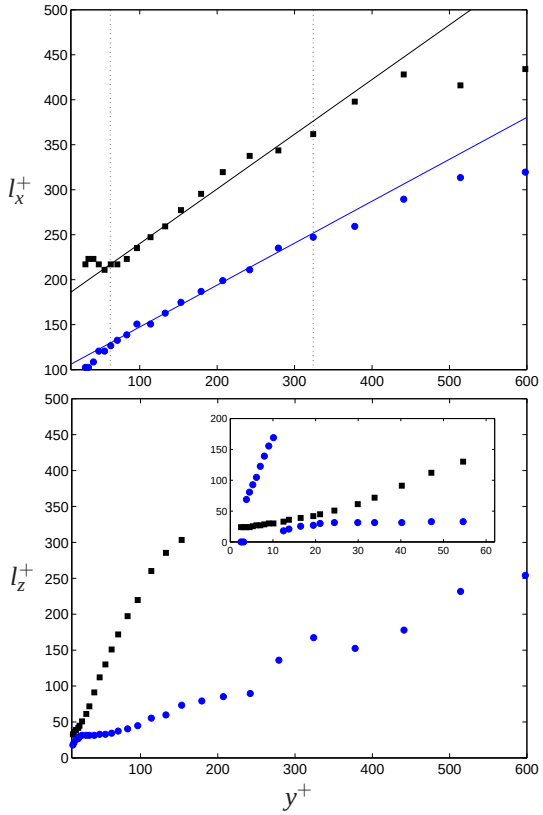

Figure 8. Streamwise, l_x^+, and spanwise, l_z^+, length scales determined from two-point velocity–vorticity correlations. ○, $\overline{v\omega_z}$; □, $\overline{w\omega_y}$. Straight lines are fitted to data in the range $y^+ = 62 - 320$ as indicated by the dotted lines.

REFERENCES

DEL ALAMO, J. C., JIMENEZ, J., ZADONADE, P. & MOSER, R. D. 2004 Scaling of the energy spectra of turbulent channels. *J. Fluid Mech.* **500**, 135–144.

AFZAL, N. 1982 Fully developed turbulent flow in a pipe: An intermediate layer. *Ing.-Arch.* **52**, 355–377.

CRAWFORD, C. & KARNIADAKIS, G. 1997 Reynolds stress analysis of EMHD-controlled wall turbulence. Part I. Streamwise forcing. *Phys. Fluids* **9**, 788–806.

EYINK G. 2008 Turbulent flow in pipes and channels as cross-stream "inverse cascades" of vorticity. *Phys. Fluids* **20**, 125101.

FIFE, P., KLEWICKI, J., MCMURTRY, P. & WEI, T. 2005 Multiscaling in the presence of indeterminacy: Wall-induced turbulence. *Multiscale Modeling and Simulation* **4**, 936–959.

FIFE, P., KLEWICKI & WEI, T. 2009 Time averaging in turbulence settings may reveal an infinite hierarchy of length scales. *J. of Discrete and Continuous Dynamical Systems*, **24**, 781–807.

KIM, K., LI, C.-F., SURESHKUMAR, R. BALACHANDAR, S. & ADRIAN, R. 2007 Effects of polymer stresses on eddy structures in drag-reduced turbulent channel flow. *J. Fluid Mech.* **584**, 281–299.

KLEWICKI, J., FIFE, P., WEI, T. & MCMURTRY, P. 2007 A physical model of the turbulent boundary layer consonant with mean momentum balance structure. *Phil. Trans. Roy. Soc. A* **365**, 823–839.

LONG, R. & CHEN, T.-C 1981 Experimental evidence for the existence of the mesolayer in turbulent systems. *J. Fluid Mech.* **105**, 19-59.

MEINHART, C., & ADRIAN, R. 1995 On the existence of uniform momentum zones in a turbulent boundary layer. *Phys. Fluids* **7**, 694–696.

PERRY, A. & CHONG, M. 1982 On the mechanism of wall turbulence. *J. Fluid Mech.* **119**, 173–217.

PERRY, A. & MARUSIC, I. 1995 A wall-wake model for the turbulence structure of boundary layers. Part 1. Extension of the attached eddy hypothesis. *J. Fluid Mech.* **298**, 361–388.

SREENIVASAN, K. & SAHAY, A. 1997 The persistence of viscous effects in the overlap region and the mean velocity in turbulent pipe and channel flows. In *Self-Sustaining Mechanisms of Wall Turbulence* (Ed. R. Panton) Computational Mechanics Publications, Southampton, 253 – 272.

TENNEKES, H & LUMLEY, J. 1972 A First Course in Turbulence. MIT Press, Cambridge.

TOWNSEND, A. 1976 The Structure of Turbulent Shear Flow. Cambridge University Press, Cambridge.

WHITE, C., DUBIEF, Y. & KLEWICKI, J. 2011 Properties of the mean momentum balance in polymer drag reduced channel flow. *J. Fluid Mech.* under-review.

GANAPATHISUBRAMANI, B. 2008 Statistical structure of momentum sources and sinks in the outer region of a turbulent boundary layer. *J. Fluid Mech.* **606**, 225–237.

GUALA, M., HOMMEMA, S. E. & ADRIAN, R. J. 2006 Large-scale and very-large-scale motions in turbulent pipe flow. *J. Fluid Mech.* **554**, 521–542.

KLEWICKI, J. C. 1989 Velocity-Vorticity correlations related to the gradients of the Reynolds stresses in parallel turbulent wall flows. *Phys. Fluids* **1(7)**, 1285–1288.

KLEWICKI, J. C. & HIRSCH, C. R. 2004 Flow field properties local to near-wall shear layers in a low Reynolds number turbulent boundary layer. *Phys. Fluids* **16(11)**, 4163–4175.

KLEWICKI, J. C., MURRAY, J. A. & FALCO, R. E. 1994 Vortical motion contributions to stress transport in turbulent boundary layers. *Phys. Fluids* **6(1)**, 277–286.

MCKEON, B. J. & SHARMA, A. S. 2011 A critical-layer model for turbulent pipe flow. *J. Fluid Mech.* **658**, 336–382.

ONG, L. 1992 Visualization of turbulent flows with simultaneous velocity and vorticity measurements. PhD thesis, University of Maryland, USA.

PRIYADARSHANA, P. J. A., KLEWICKI, J. C., TREAT, S. & FOSS, J. 2007 Statistical structure of turbulent boundary layer velocity-vorticity products at high and low Reynolds numbers. *J. Fluid Mech.* **570**, 307–346.

RAJAGOPALAN, S. & ANTONIA, R. A. 1993 Structure of the velocity field associated with the spanwise vorticity in the wall region of a turbulent boundary layer. *Phys. Fluids* **5(10)**, 2502–2510.

ROVELSTADT, A. L. 1991 Lagrangian analysis of vorticity transport in a numerically simulated turbulent channel flow. PhD thesis, University of Maryland, USA.

WEI, T., FIFE, P., KLEWICKI, J. C. & MCMURTRY, P. 2005 Properties of mean momentum balance in turbulent boundary layer, channel and pipe flows. *J. Fluid Mech.* **522**, 303–327.